# Dynamic Response of Aircraft Autopilot Systems to Atmospheric Disturbances

R. John Hansman Jr.* and James L. Sturdy†
*Massachusetts Institute of Technology, Cambridge, Massachusetts*

**The dynamic response of aircraft autopilot systems to atmospheric disturbances was investigated by analyzing linearized models of aircraft dynamics and altitude-hold autopilots. Three transport category aircraft (Boeing 737-100, McDonald–Douglas DC 9-30, and Lockheed L-1011) were studied at three flight levels (FL290, FL330, and FL370). The models were analyzed to determine the extent to which pressure surface fluctuations, vertical gusts, and horizontal gusts cause dynamic altitude errors by coupling with the aircraft autopilot dynamics. The results of this analysis were examined in light of meteorological data on disturbance magnitudes and wavelengths collected from observations of mountain wave activity. This examination revealed that atmospheric conditions do exist that can cause aircraft to exhibit dynamic altitude errors in excess of 1000 ft. Pressure surface fluctuations were observed to be the dominant source of altitude errors in flights through extreme mountain wave activity. Based on the linear analysis, the maximum tolerable pressure surface fluctuation amplitude was determined as a function of wavelength for an allowable altitude error margin. The results of this analysis provide guidance for the determination of vertical separation standards in the presence of atmospheric disturbances.**

## Nomenclature

$f$ = apparent frequency of disturbance
$h$ = aircraft altitude
$\dot{h}$ = aircraft vertical velocity
$\ddot{h}$ = aircraft vertical acceleration
$h_c$ = commanded altitude
$h_p$ = amplitude of pressure surface fluctuation
$q$ = aircraft pitch rate
$S$ = Laplace transform variable
$U$ = amplitude of horizontal gust
$V$ = ground speed of aircraft
$W$ = amplitude of vertical gust
$\delta_{e_c}$ = commanded elevator deflection
$\Delta h$ = amplitude of altitude error
$\lambda$ = wavelength of disturbance measured along flightpath
$\theta$ = aircraft pitch angle
$\theta_c$ = commanded pitch angle

## I. Introduction

In recent years changes have been proposed to the international vertical separation standards that would reduce the minimum altitude separation for aircraft in level flight above 29,000 ft (FL290) from 2000 to 1000 ft. The current separation standard at altitudes below FL290 is 1000 ft. Motivation for this change comes from the improvements in altimetry system accuracy, which have been made since the mid-fifties when the current standard went into effect, and the potential benefits of increasing the number of usable flight levels. These benefits include: increased flexibility in air traffic control (ATC) routing; increased throughput at high altitudes; and fuel conservation through allowing more aircraft to fly near their most efficient altitudes.

Received Dec. 3, 1987; presented as Paper 88-0578 at the AIAA 26th Aerospace Sciences Meeting, Reno, NV, Jan. 11-14, 1988; revision received April 15, 1988. 

*Associate Professor, Aeronautics and Astronautics. Member AIAA.

†Research Assistant, Aeronautics and Astronautics; presently with MIT Lincoln Laboratory.

The separation standard defines the minimum vertical spacing that is allowed between aircraft flying in the vicinity of each other. Because aircraft altimetry systems are based on pressure measurement and assume the standard atmosphere, air traffic assignments to fly at a constant flight level actually correspond to flying a surface of constant barometric pressure. Because of inherent errors involved in trying to track a given pressure surface, the separation standard was introduced to ensure the safety of aircraft flying in the vicinity of each other. The magnitude of these tracking errors, as illustrated in Fig. 1, is the difference between the aircraft's assigned and actual pressure altitude. The magnitude of these errors is a primary factor in determining the minimum vertical spacing that can be safely used.

Most recent studies of altimetry precision[1] have focused on error sources in the altimetry and static pressure systems, which are used to measure barometric pressure on board the aircraft. These error sources, which include such factors as calibration error, hysteresis in the pressure transducer, pressure leaks, and static position error, result primarily in a constant offset. This results in the aircraft tending to fly at a fixed increment above or below its assigned altitude.

In addition to the constant offset error sources described above, evidence has been obtained by monitoring the mode C altitude-reporting transponder output of commercial, military, and general aviation aircraft, which indicates that significant dynamic altitude deviations also occur. An example of such an occurrence is presented in Fig. 2. The mode C data in this figure indicates a 700-ft deviation for a twin-engine Saberliner jet aircraft flying at FL370 with its altitude-hold autopilot engaged during a period of reported mountain wave activity in the Denver, Colorado, area. Note that this large deviation occurs during a period of apparently unsteady flight.

In this study, the magnitude of dynamic errors that result from the inability of aircraft to hold constant pressure altitudes in the presence of strong atmospheric disturbances was assessed. This inability to track altitude is due primarily to the physical (aerodynamic, structural, and control) limitations on the aircraft's performance. The analysis was limited to flight with an altitude hold autopilot engaged because this is the normal procedure in cruise flight and because the autopilot response can be modeled accurately. Disturbances investigated include: fluctuations in the height of the constant pressure sur-

face (such as those depicted in Fig. 1), vertical gusts, and horizontal gusts.

## II. Analytical Approach

### A. Model Synthesis

This study involved the analysis of linearized models of the longitudinal dynamics for several aircraft at specific altitudes. These models typically involve such flight parameters as longitudinal and vertical velocities, pitch angle, and pitch rate, with each parameter being expressed as a deviation from its value in level flight at the specific altitude. Each linear model was expanded to generate values for the aircraft's altitude, altitude rate, and vertical acceleration, when required. The expanded aircraft model was then integrated with a typical linear autopilot model for that aircraft. This yielded a full model of the closed-loop aircraft-autopilot system. In the analysis, an ideal altimetry system was assumed. Provisions were made to introduce pressure surface fluctuations as well as vertical and horizontal gusts into the system as disturbances.

### B. Method of Analysis

The effect of each disturbance on the aircraft's altitude-tracking accuracy was evaluated by using the closed-loop models to generate power spectral density plots.[2] The power spectral density plot is a measure of a system's frequency response to a given disturbance. A property of linear systems (and linearized models) is that when they are excited by a sinusoidal input or disturbance of a given frequency, the output will be a sinusoid of the same frequency but usually of a different amplitude and phase. As an example, typical patterns of aircraft response to sinusoidal pressure surface fluctuations are shown in Figs. 3–5 for a model of a Boeing 737-100 at FL330. The three cases presented are examples of low, moderate, and high frequency fluctuations. (Note that the frequency can be converted to a wavelength $\lambda$ through the relation: $\lambda = V/f$, where $V$ is the aircraft's inertial velocity. $V$ was typically between 780 and 800 fps for the aircraft in this study.) For each frequency, the first plot depicts the aircraft's trajectory and the desired pressure surface. The second plot indicates the time varying altitude tracking error. Note that both the magnitude of the altitude error and its phase shift relative to the disturbance vary with the frequency of the disturbance.

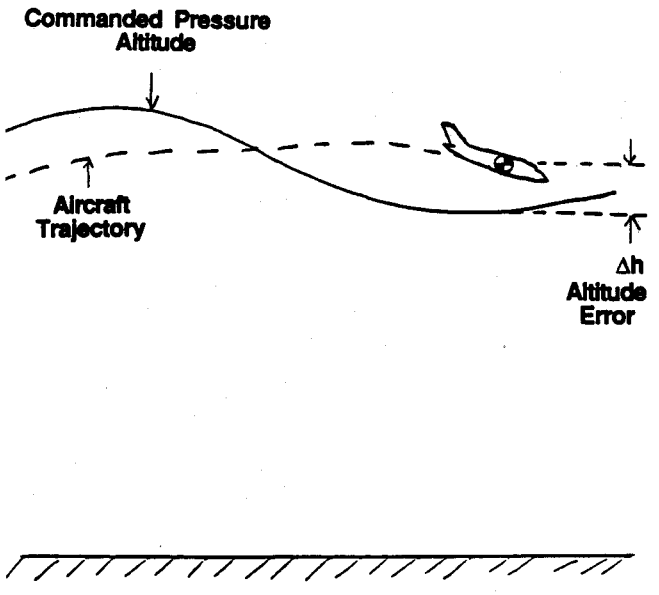


Fig. 1 Definition of altitude error ($\Delta h$).

Since this analysis is concerned with the magnitude of altitude errors, as opposed to phase relationships, the power spectral density plot is used instead of the more common Bode plots to illustrate sensitivity of dynamic errors to disturbances. The power spectral density (PSD) plot is a graph of the ratio of the mean-squared output (altitude error) to the mean-squared input (disturbance) vs frequency. For linear systems, the PSD is also the squared ratio of the amplitude of the sinusoidal output (altitude error) to the amplitude of the sinusoidal input (disturbance). Figure 6 shows the power spectral density for the aircraft-autopilot system used to generate the trajectories in Figs. 3–5. Note that the three points indicated on the PSD curve are at the frequencies used in the above trajectories. The low-frequency example can be seen to have a low PSD value corresponding to the small tracking error. The high-frequency example has a PSD value of unity since the altitude error is essentially equal to the disturbance magnitude.

### C. Description of Aircraft

To date, three aircraft have been studied: a Boeing 737-100, a McDonald–Douglas DC 9-30, and a Lockheed L-1011. All three are commercial aircraft certified under Federal Aviation Regulations (FAR) Part 25. These aircraft were chosen because they represent a spectrum of transport category aircraft for which stability and autopilot data were available.[3] The

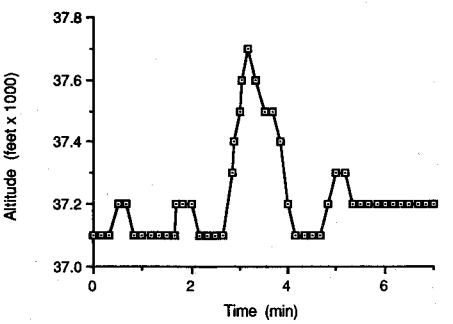


Fig. 2 Mode C data recorded during a mountain wave encounter showing an altitude deviation of 700 ft.

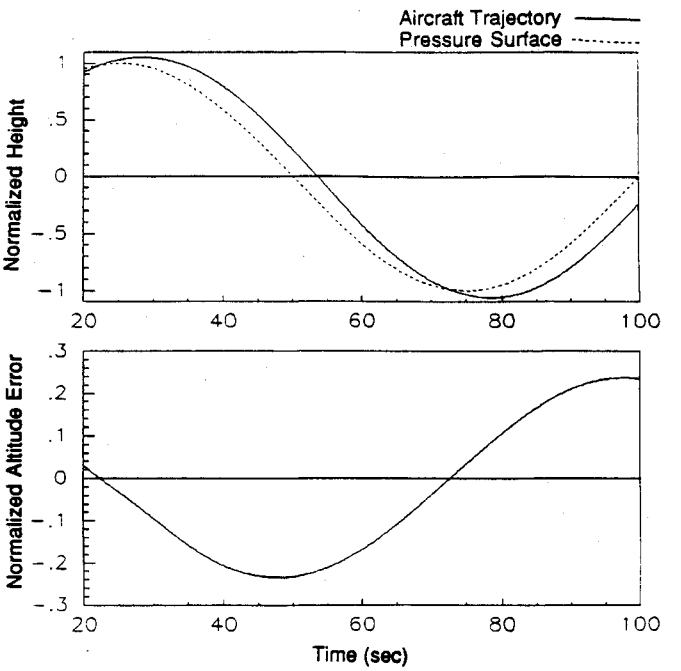


Fig. 3 Aircraft response to low-frequency pressure surface fluctuations (normalized to the vertical displacement amplitude of the pressure surface).

analysis for each aircraft has been carried out for flight at three altitudes (FL290, FL330, and FL370) and at a Mach number of 0.8. The DC 9-30 aircraft had insufficient thrust to reach FL370 at the weight for which the linear model was generated and was therefore evaluated at FL357 instead. Unless otherwise noted, the data that follows will correspond to FL330.

The open-loop behavior of all three aircraft is similar. Each exhibits a lightly damped, long-period oscillatory behavior, the phugoid mode, during which the aircraft slowly rises and sinks, exchanging kinetic and potential energy. For the DC 9-30 aircraft, this mode has a period of about 105 s and a damping ratio of 0.23. Although it is a larger aircraft, the L-1011 oscillates at a higher frequency (75-s period) and has a lower damping ratio (0.09). The 737 oscillates at an even higher frequency than the L-1011 (63-s period) and has a damping ratio of 0.034.

The autopilots for each aircraft are depicted in block-diagram form in Figs. 7–9, and are relatively similar to each other in form. Each has an inner feedback loop that uses measurements of pitch angle and pitch rate to control the aircraft's pitch angle. An altitude-tracking outer feedback loop uses measurements of the aircraft's altitude error and vertical velocity to generate a pitch angle command for the inner loop. The outer loop in the L-1011 also uses vertical acceleration information.

## III. Sensitivity to Atmospheric Disturbances

### A. Pressure Surface Fluctuations

The sensitivity of each aircraft to fluctuations in the height of the FL330 pressure surface is indicated by the power spectral density plots in Fig. 10. The closed-loop behavior of the three aircraft is quite similar despite the variations in their open-loop behavior mentioned in Sec. IIc. This is most likely the result of similar design objectives for each autopilot. At low frequencies, the low error values indicate that for these disturbances the autopilot is capable of keeping the aircraft at its proper altitude. This low frequency behavior is illustrated in Fig. 3 for the 737-100 at FL330. The aircraft trajectory closely follows the pressure surface with only a slight phase lag, and the altitude error is small.

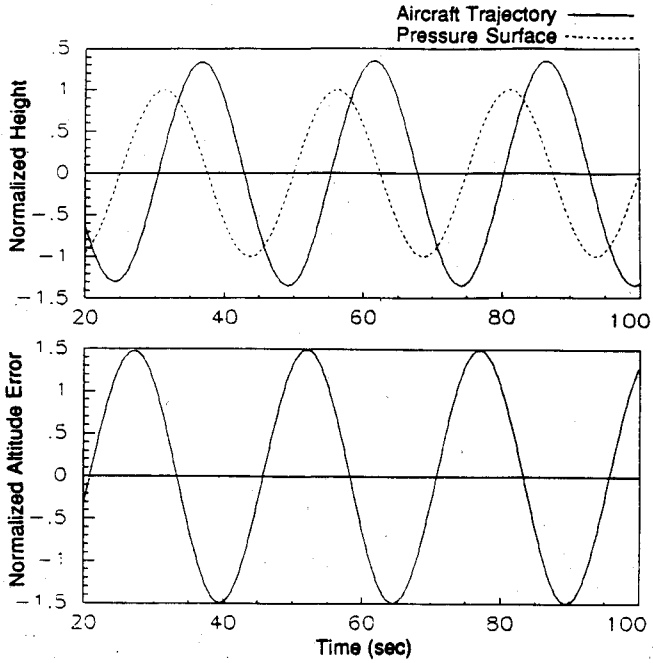


Fig. 4 Aircraft response to midfrequency pressure surface fluctuations (normalized to the vertical displacement amplitude of the pressure surface).

At higher frequencies, the three curves approach unity because the aircraft-autopilot system cannot respond to these fast disturbances. As illustrated in Fig. 5, the aircraft tends to ignore high-frequency disturbances and fly at a relatively constant level. The altitude error is, therefore, approximately equal in magnitude to the pressure surface fluctuation. The severity of the high-frequency error is exaggerated in the power spectral density representation due to the assumption of uniform disturbance magnitudes at all frequencies. Actual pressure surface fluctuation magnitudes will tend to decrease at higher frequencies, thereby limiting the high-frequency error.

In the midfrequency region, each aircraft exhibits a peak sensitivity. This peak, which is most severe for the Boeing 737-

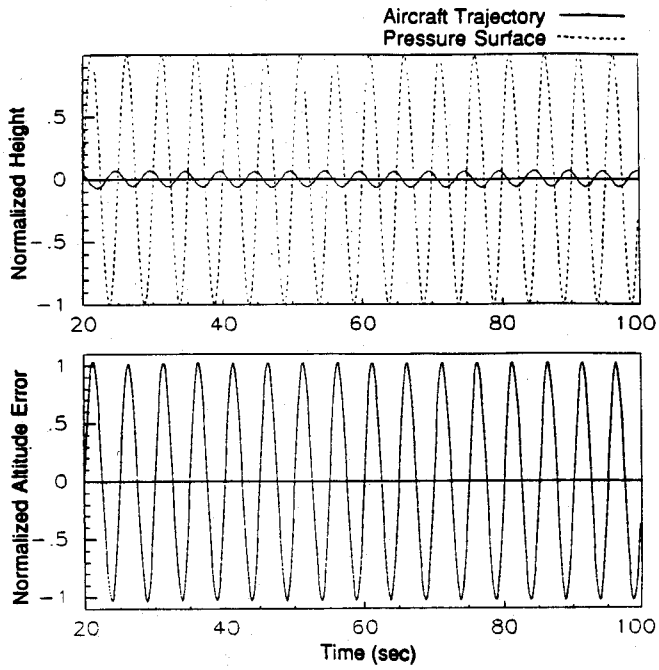


Fig. 5 Aircraft response to high-frequency pressure surface fluctuations (normalized to the vertical displacement amplitude of the pressure surface).

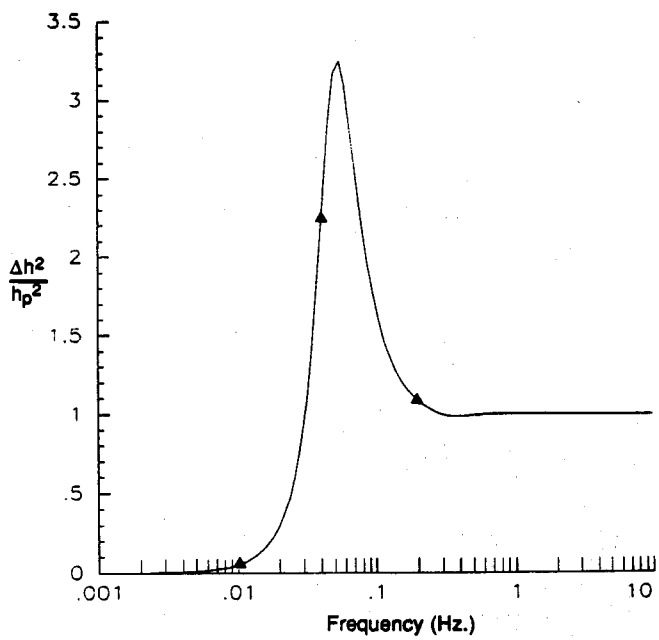


Fig. 6 Altitude error sensitivity to pressure surface fluctuations for Boeing 737-100.

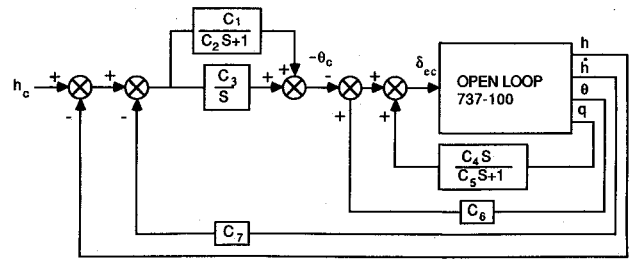


Fig. 7 Block diagram of autopilot for the Boeing 737-100.

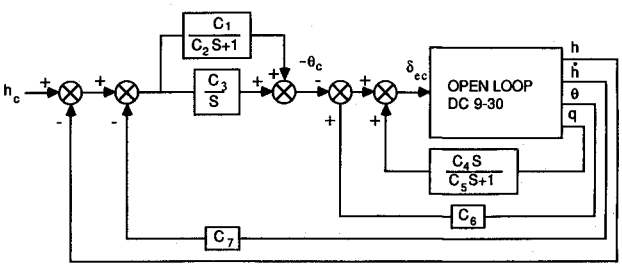


Fig. 8 Block diagram of autopilot for the McDonald–Douglas DC 9-30.

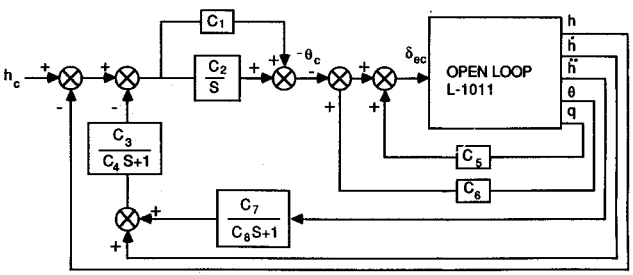


Fig. 9 Block diagram of autopilot for the Lockheed L-1011.

100, is a result of the disturbance driving the closed-loop aircraft-autopilot system at resonance. As can be seen in Fig. 4, the autopilot attempts to make the aircraft follow the pressure surface. The effective inertia of the aircraft, however, causes the aircraft to be significantly out of phase with the pressure surface in this frequency range. The net result is that the magnitude of the altitude error actually exceeds that of the input disturbance in this region.

### B. Vertical Gusts

The sensitivity of each aircraft to vertical gusts is demonstrated by the PSD plots in Fig. 11. Since these plots relate altitude errors to air velocities, the ratio of squared amplitudes cannot be expressed in nondimensional form. In the analysis of gust disturbances, the PSD plots are measured in units of $s^2$. Therefore, wind inputs in units of ft/s would result in error outputs in units of feet. Although the trends are the same for each aircraft, the magnitude of the resonance peaks differs greatly. At relatively low frequencies, the aircraft are able to track the desired altitude fairly well. At high frequencies, the inertia of the aircraft tends to limit the effect of the vertical gusts, and the sensitivity is again small. In the midfrequency range, however, there appears to be a fair amount of coupling between the vertical gusts and the dynamics of the closed-loop aircraft-autopilot system. This coupling results in a resonance peak that is observed to be at a slightly lower frequency of peak sensitivity to pressure surface fluctuations. Care should be exercised in comparing the gust power spectral density values to pressure values due to the dimensional dissimilarity.

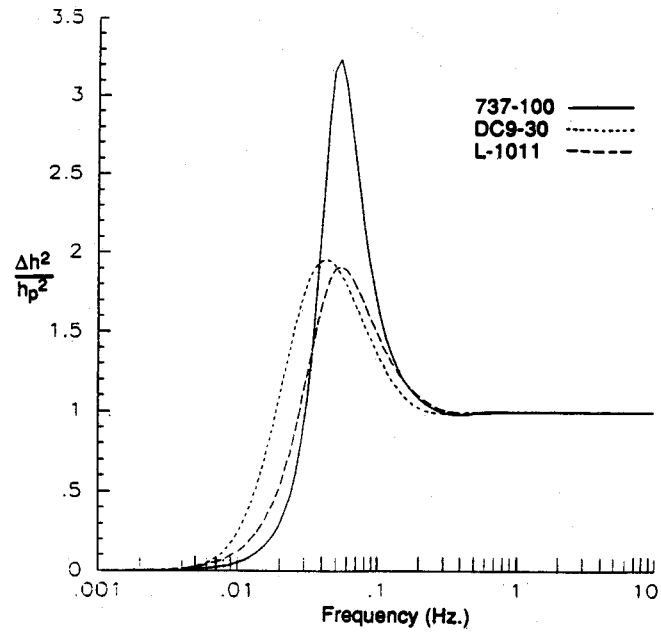


Fig. 10 Altitude error sensitivity to pressure surface fluctuations.

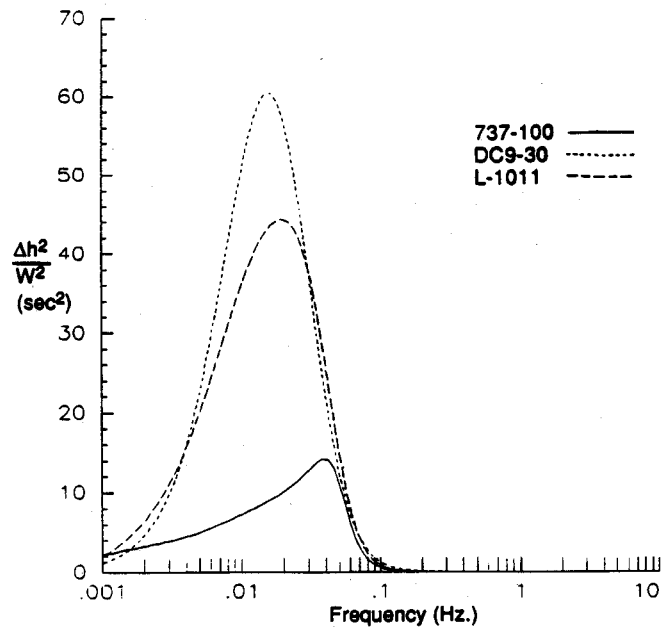


Fig. 11 Altitude error sensitivity to vertical gusts.

### C. Horizontal Gusts

Figure 12 indicates the sensitivity of each aircraft to longitudinal horizontal gusts (i.e., headwind-tailwind). The reaction of the aircraft to horizontal gusts is similar to their reaction to vertical gusts in both the shape of the curve and the frequency at which the peak sensitivity occurs for each. All three aircraft exhibit less sensitivity to horizontal gusts than to vertical gusts of equal magnitude. This is due to the vertical gusts directly affecting the aircraft's altitude, whereas the horizontal gusts indirectly affect altitude through airspeed-altitude coupling.

### D. Effect of Altitude

The sensitivity of the Boeing 737-100 to the three types of disturbances is shown in Figs. 13–15 for flight at FL290, FL330, and FL370. Although there is some variation in the aircraft's sensitivity at different altitudes, the variation is relatively small, and the overall trends remain the same. The

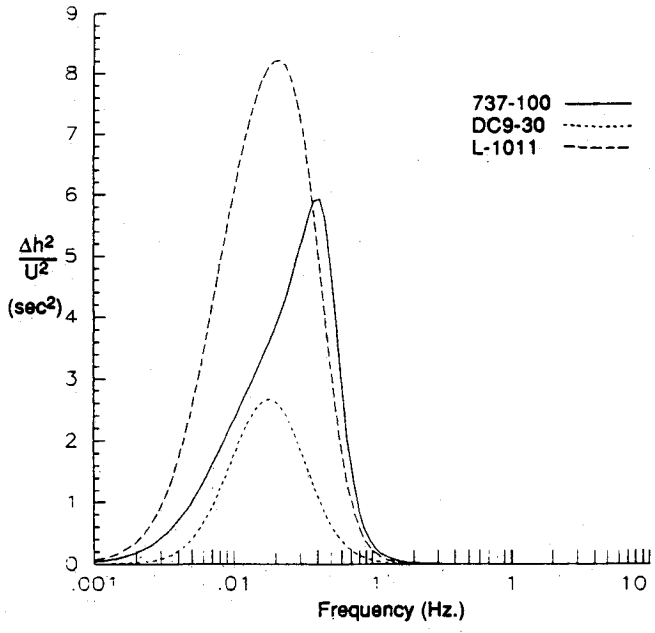


Fig. 12 Altitude error sensitivity to horizontal gusts.

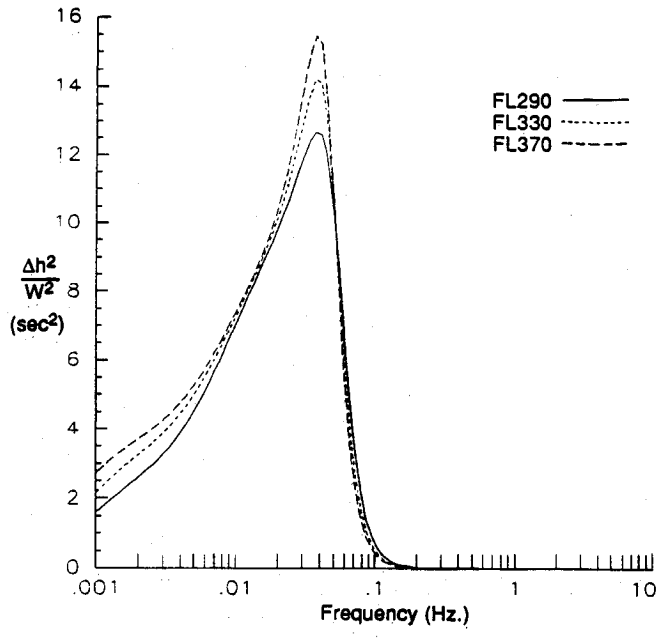


Fig. 14 Altitude error sensitivity to vertical gusts for the Boeing 737-100 at three flight levels.

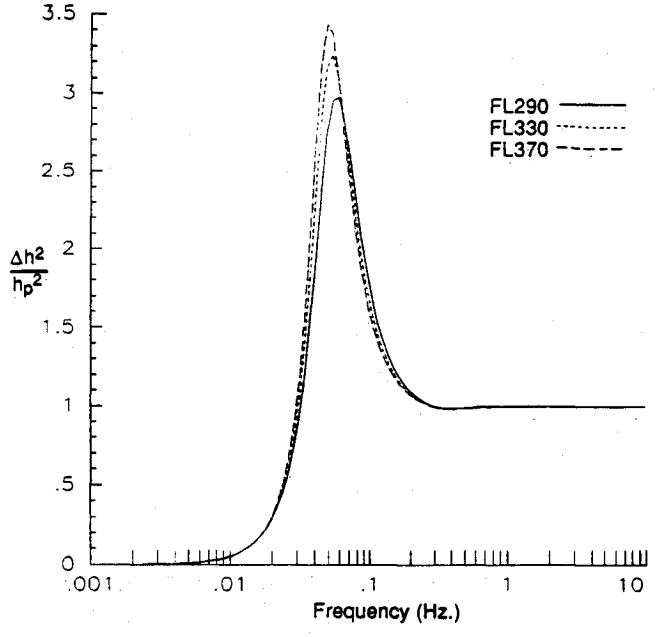


Fig. 13 Altitude error sensitivity to pressure surface fluctuations for the Boeing 737-100 at three flight levels.

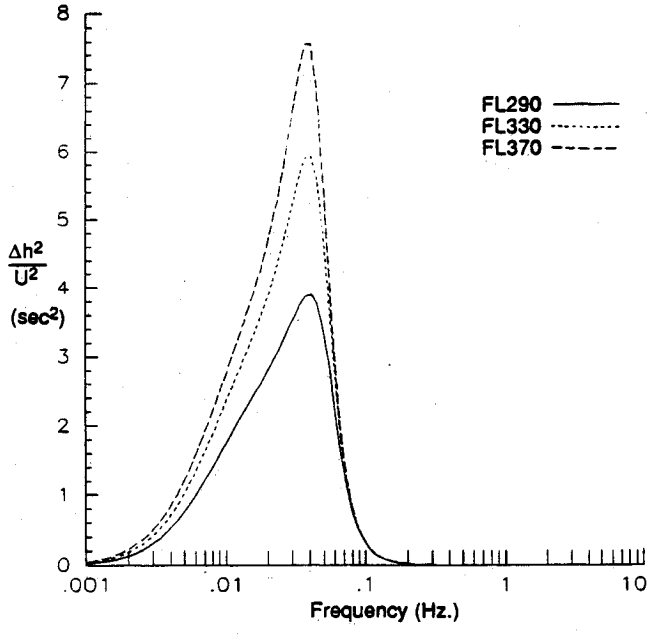


Fig. 15 Altitude error sensitivity to horizontal gusts for the Boeing 737-100 at three flight levels.

analysis of the DC 9-30 and the L-1011 aircraft also shows that their behavior does not differ significantly with altitude at these flight levels.

## IV. Implications for High-Altitude Wave Encounters

The potential sources of large-magnitude atmospheric disturbances observed to be important to the dynamics of altitude tracking are: 1) waves that form in the lee of mountains, and 2) gravity shear waves which can form typically at the edge of the jetstream. Figures 16 and 17 indicate observed pressure surface fluctuation and vertical gust magnitudes for mountain waves plotted against their observed wavelengths as compiled by Atkinson.[4] This data was obtained from a variety of meteorological studies including aircraft penetrations, surface pressure measurements, and radar and satellite observations. Consequently, the data represent a variety of flight levels. In addition, there is some uncertainty in the meteorological data due to the nature of the observations. Several extremely large amplitude cases which were well outside the data cluster have therefore been omitted in Figs. 16 and 17.

The meteorological data can be examined in the context of the PSDs given above. An example is shown in Fig. 18 which plots the expected error amplitude for the DC 9-30 aircraft subject to the mountain wave pressure fluctuations and vertical gusts reported in Figs. 16 and 17. The DC 9-30 aircraft is presented because it shows the greatest sensitivity to vertical gusts. It is apparent that pressure surface fluctuations are reported which would result in altitude errors in excess of 1000 ft if encountered by any of the three aircraft studied. It is also clear that the altitude errors, which could result from the more

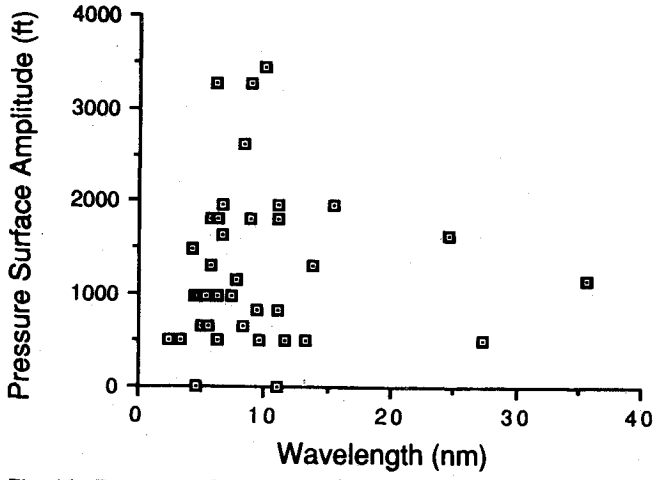


Fig. 16 Pressure surface fluctuation amplitudes and wavelengths observed in mountain waves as reported by Atkinson.[4]

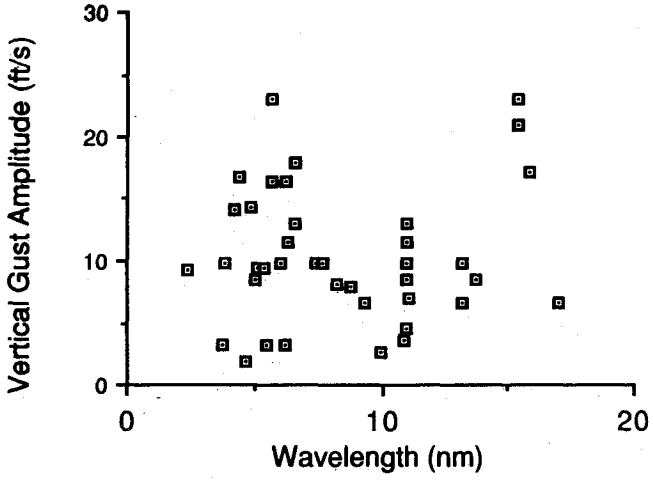


Fig. 17 Vertical gust amplitudes and wavelengths observed in mountain waves as reported by Atkinson.[4]

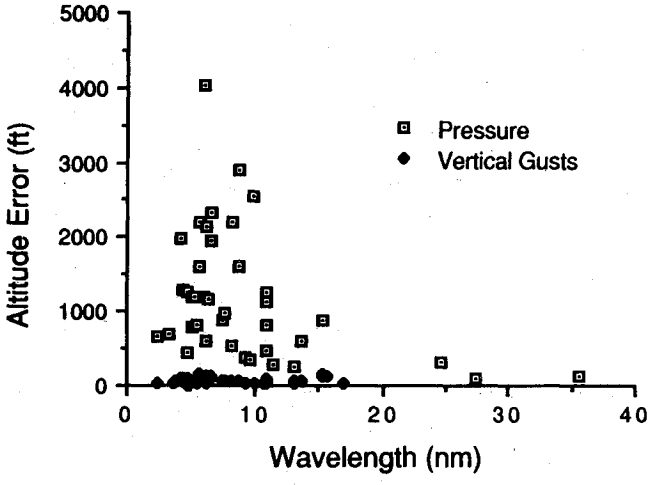


Fig. 18 DC 9-30 altitude error resulting from observed pressure surface fluctuations and vertical gusts reported by Atkinson.[4]

severe pressure fluctuations, are a factor of 10 or more larger than the altitude errors that could result from the more severe vertical gusts. This implies that pressure surface fluctuations are the primary cause of altitude tracking error in severe mountain wave encounters.

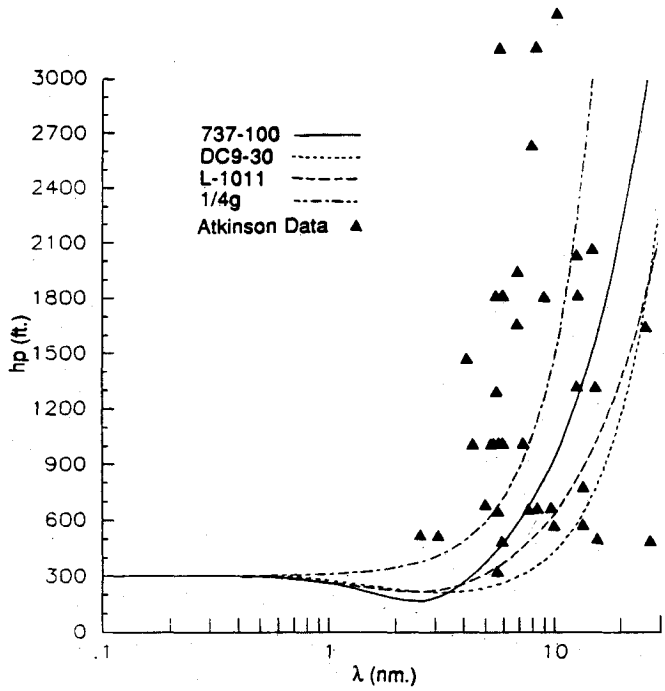


Fig. 19 Tolerable pressure surface fluctuations for a specified altitude error limit of 300 ft.

## V. Determination of Critical Pressure Surface Fluctuation Amplitudes

Since pressure surface fluctuations have been determined to be the primary cause of altitude-tracking error in mountain wave encounters, it is reasonable to identify critical pressure surface fluctuation amplitudes. This is accomplished by inverting the pressure surface fluctuation PSD results. By doing this, a threshold magnitude of pressure surface fluctuation as a function of wavelength can be established beyond which each aircraft will deviate from its assigned altitude by more than a specified error margin for at least part of its oscillatory cycle. Figure 19 shows the results of such an analysis for each of the three aircraft studied with a specified error margin of 300 ft. The 300-ft value is thought to be representative of the maximum allowable deviation in a 1000-ft vertical separation environment. A plot representing the optimum performance for any aircraft if vertical accelerations are limited to plus or minus 1/4 $g$ is also included for reference. Superimposed on this figure is the Atkinson data on observed pressure surface fluctuations. It is readily seen that many of the observed mountain waves would cause all of the aircraft to exhibit altitude deviations well in excess of 300 ft.

## VI. Conclusions

Based on the above analysis the following observations were made:

1) Atmospheric conditions do occur which can cause aircraft to exhibit significant assigned altitude deviations due to aircraft-autopilot system dynamics.

2) The effect of atmospheric disturbances is strongest when they couple in frequency with the dynamics of the aircraft-autopilot system.

3) Analysis of available meteorological data suggests that fluctuations in the height of the pressure surface tend to be the largest source of altitude errors for flights.

4) If the aircraft-autopilot dynamics are known, a maximum amplitude of pressure surface fluctuation can be defined for any wavelength such that the aircraft will remain within a specified margin of its assigned altitude upon encountering such a disturbance.

5) Additional meteorological data is required to assess the

probability of an aircraft exhibiting a significant altitude deviation due to atmospheric disturbances.

The results of this work should help in identifying which meteorological data must be examined in order to determine the viability of reducing vertical separation standards and in determining which data would cause aircraft to exhibit significant altitude deviations.

## Acknowledgments

This work was sponsored by the Federal Aviation Administration under Contract DTFA03-86-C-00016. The work was also supported by the NASA–Federal Aviation Administration Joint University Program, Grant NGL-22-009-640, as well as the National Science Foundation Presidential Young Investigators Award Program, Award 8552702. Aircraft and autopilot data were provided by Richard Huschen of the NASA Langley Research Center.

## References

[1]Gracey, W., *The Measurement of Aircraft Speed and Altitude*, NASA Reference Publication 1046, Langley Research Center, Hampton, VA, 1980.

[2]Brown, R. G., *Introduction to Random Signal Analysis and Kalman Filtering*, John Wiley & Sons, New York, 1983, pp. 83–84.

[3]Hueschen, R. M., Aerospace Technologist, personal communications, 1987.

[4]Atkinson, B. W., *Meso Scale Atmospheric Circulations*, Academic Press, New York, 1981, pp. 36–37.